44. Value used in (*45*) for a corn-based ethanol plant; believed to be conservative for an economical cellulose-to-ethanol process.
45. R. S. Chambers, R. A. Herendeen, J. J. Joyce, P. S. Penner, *Science* **206**, 789 (1979).
46. M. A. Johnson, *Energy* **8**, 225 (1983); J. M. Krochta, in *Proceedings of the Second International Conference on Energy Use Management* (Pergamon, Elansford, NY, 1979), pp. 1956–1963); F. Parisi, *Adv. Biochem. Eng.-Biotechnol.* **28**, 41 (1983); T. Yorifugi, *Energy Dev. J.* **3**, 195 (1981).
47. Based on heat of combustion for petroleum liquids [*Basic Pet. Data Book* [(American Petroleum Institute, Washington, DC, 1989), vol. 9, no. 3], adding 19% for oil recovery, refining, and distribution (*40*).
48. R. C. Loehr and M. Sengupta, *Environ. Sanit. Rev.* **16** (1985); E. D. Waits and J. L. Elmore, *Environ. Int.* **9**, 325 (1983).
49. Threshold Limit Values for Chemical Substances and Physical Agents in the Workman Environment with Intended Changes for 1980s (American Conference of Government Industrial Hygienists, Cincinnati, OH, 1980).
50. *Hydrocarb. Process.* **68** (no. 11), 85 (1989); *ibid.* **67** (no. 9), 61 (1988).
51. L. R. Lynd, *Appl. Biochem. Biotechnol.* **24/25**, 695 (1990).
52. M. K. Veldhuis, L. M. Christensen, E. I. Fulmer, *Ind. Eng. Chem.* **28**, 430 (1936); T. K. Ng, P. J. Weimer, J. G. Zeikus, *Arch. Microbiol.* **114**, 1 (1977).
53. L. R. Lynd, H. E. Grethlein, R. H. Wolkin, *Appl. Environ. Microbiol.* **55**, 3131 (1989).
54. J. N. Van Arsdell *et al.*, *Bio/Technology* **5**, 60 (1987); B. Surbriggen, M. J. Bailey, M. E. Penttila, K. Poutanen, M. Linko, *J. Biotechnol.* **13**, 267 (1990); M. E. Penttila, P. Lehtovaara, M. Bailey, T. T. Teeri, J. K. C. Knowles, *Gene* **63**, 103 (1988).
55. *National Assessment of Undiscovered Conventional Oil and Gas Resources, Working-Paper* (Working pap., U.S. Geological Survey and Minerals Management Service, March 1989); R. A. Kerr, *Science* **245**, 1330 (1989).
56. M. Grathwohl, *World Energy Supply* (de Gruyter, Berlin, 1982).
57. L. R. Lynd, *Adv. Biochem. Eng.-Biotechnol.* **38**, 1 (1989).
58. The indicated range is consistent with the evaluation of the DOE Biofuels Feedstock Development Program [R. D. Perlack and J. W. Ranney, *Energy* **12** (no. 12), 1217 (1987); (*35*)].
59. S. Kane, J. Reilly, M. LeBlanc, J. Hrubovcak, *Agribusiness* **5**, 505 (1989); *Feed Situation and Outlook Report* (USDA, FDS-314, Washington, DC, 1990).
60. C. E. Wyman and N. D. Himman, *Appl. Biochem. Biotechnol.* **24/25**, 735 (1990).
61. J. D. Ferchak and E. K. Pye, *Sol. Energy* **26**, 9 (1981); J. W. Ranney, L. L. Wright, P. A. Layton, *J. For.* **85** (no. 8), 17 (1987); N. Smith and T. J. Corcoran, *Am. Chem. Soc. Symp. Ser.* **144**, 433 (1981).
62. G. Marland and A. Turhollow, *Oak Ridge Natl. Lab. Environ. Sci. Div. Publ. 3301* (1990).
63. *Agricultural Resources—Cropland, Water, and Conservation, Situational Outlook and Report* (USDA, Washington, DC, 1988).
64. "Basic Statistics, 1982 National Resources Inventory," *USDA Soil Conserv. Serv. Stat. Bull. 756* (1987).
65. H. E. Grethlein, D. C. Allen, A. O. Converse, *Biotechnol. Bioeng.* **26**, 1498 (1984).
66. We thank M. DeLuchi, P. Lorang, R. Moorer, and A. Turhollow for useful discussions and information. Publication 3644, Environmental Sciences Division, Oak Ridge National Laboratory.

Why Gases Dissolve in Liquids

GERALD L. POLLACK

The thermodynamics and statistical mechanics of solubility are fairly well understood. It is still very difficult, however, to make quantitative predictions of solubility for real systems from first principles. The purposes of this article are to present the results of solubility experiments in some prototype solute-solvent systems, to show how far they may be understood from molecular first principles, and to discuss some of the things that are still missing. The main systems used as examples have the inert gas xenon as solute and some simple organic liquids as solvents.

ALL GASES DISSOLVE IN ALL LIQUIDS, BUT THE ACTUAL solubilities range over many orders of magnitude. For inert gases at room temperature, for example, the solubility of Xe in *n*-octane, a common hydrocarbon liquid, is 470 times that of He in water. Gas solubility can vary much more for complex solutes and solvents. As an example, the solubility of the anesthetic gas halothane in olive oil is more than 10^6 times the solubility of common gases in liquid mercury.

Can the solubilities of gases in liquids be quantitatively understood from molecular first principles? The question can be generalized with the help of the Gibbs phase rule, according to which systems such as these with two components and two phases have two degrees of freedom, such as temperature and pressure. Therefore, the question may be enlarged to include: Can the temperature and pressure dependence of these solubilities be understood from molecular first principles?

The author is in the Department of Physics and Astronomy, Michigan State University, East Lansing, MI 48824.

One purpose of this article is to discuss how far we can go, using current experiments and modern theory, in answering these questions. Also discussed with the same ideas are some applications of solubility. Finally, there are some suggestions of what natural next steps would advance our understanding of the subject.

Solubility is an old subject, although most of the early interest was in solubility of solids in water, which is still an important area of research and applications. Aristotle knew that evaporation of seawater would recover dissolved salts, and there are records of a systematic study by Pliny the Elder of the relative solubilities of many solids in water.

Early quantitative measurements of the solubility of gases, a more difficult measurement, were made by William Henry (*1*), as well as by Cavendish, Priestley, and others. Henry studied the pressure and temperature dependence of air, H_2, N_2, O_2, and other gases in water. He discovered, among other things, that O_2 is more soluble than N_2 in water. This is an early example of the principle that is the basis of preferential extraction of one gas from a mixture of gases by use of a solvent. Since that time, the subject has been actively studied because of its fundamental interest and applications. More recently, extensive contributions to understanding gas solubility have been made by Hildebrand and his co-workers and by many others (*2, 3*). Review articles give comprehensive discussions of the subject as well as results for many solute-gas, solvent-liquid systems (*4, 5*).

Ostwald solubility (L) is an especially useful and also intuitive measure of gas solubility (*6*). It is defined as the ratio of the concentration of gas molecules dissolved at equilibrium in the liquid solvent to their concentration in the gas phase. In other words, L is the ratio: (moles of solute per liter of solution)/(moles of solute per liter of gas). We then can write

$$L = \rho_2^{\ell}/\rho_2^{g} \quad (1)$$

where ρ is the number density and subscripts 1 and 2 stand for, respectively, solvent and solute.

Figure 1 is a schematic representation of Ostwald solubility for Xe gas in two solvents. Ostwald solubility depends on temperature, that is, $L = L(T)$. However, at low pressures, up to a few atmospheres, it usually does not depend sensitively on pressure; that is a consequence of Henry's law (*1*). In this article I shall discuss mainly temperature dependence of solubility. Pressure dependence is an important large subject of its own (*7, 8*).

Figure 2 shows the temperature dependence of solubility for some nonreacting gases in water and in *n*-octane. Figure 2A shows that for O_2 and Xe in water the solubilities decrease as the temperature increases; this is the behavior we normally expect. Moreover, the solubilities of Ar and H_2 in *n*-octane increase as temperature increases (Fig. 2A), a somewhat counterintuitive behavior. For the four gas-water systems shown in Fig. 2B, $L(T)$ has a minimum, that is, it decreases and then increases. We shall see later how these behaviors depend on microscopic quantities.

Some representative values of Ostwald and mole fraction solubilities are shown in Tables 1 and 2. The mole fraction solubilities (x_2) refer to the fraction of solute dissolved in the solvents in equilibrium with a partial pressure of 1 atm of solute gas. It is clear from these tables that L can be greater or less than one. Mole fraction solubilities are by definition less than one. However, for nonreacting gases they are generally much less than one. The logarithm of L is related to the work required to put a solute molecule into the solvent. The consequences of this relation are discussed below.

Applications

In this section I briefly discuss some, eclectically chosen but representative, applications of gas solubility. Several of these depend on the property that nonpolar, nonreacting gases tend to concentrate in nonpolar liquids such as hydrocarbons, their derivatives, and oils, compared to water and aqueous solutions.

The volume partition coefficient, or relative solubility, of Xe between *n*-octane and water at 20°C is 37 (Fig. 1). Other simple solute gases behave in a similar way, that is, their equilibrium concentrations in nonpolar solvents are higher, sometimes much higher, than in water. Thus, for example, at 25°C: $L(N_2$ in octane$)/L(N_2$ in water$) = 12$, $L(O_2$ in octane$)/L(O_2$ in water$) = 10$, $L(H_2$ in octane$)/L(H_2$ in water$) = 5.4$, and L(He in octane$)/L$(He in water$) = 3.8$ (*5, 9*). The logarithm of these ratios of Ostwald solubilities is a measure, at fixed temperature, of what is called the excess chemical potential difference between atoms dissolved in the two solvents. This quantity will be discussed later. A rough general rule is that, as the solute becomes smaller and less polarizable (say, in the direction Xe to He), its solubility in liquids decreases. The partition coefficient between nonpolar and polar liquids also decreases but remains greater than one.

Table 1. Some representative Ostwald and mole fraction solubilities of noninteracting gases in water and in *n*-octane. The mole fraction solubility x_2 is the equilibrium mole fraction of solute in the solution, $x_2 = \rho_2^{\ell}/(\rho_1^{\ell} + \rho_2^{\ell})$, at 1 atm partial pressure of solute gas. Data are from (*5, 9*).

Solubility system (solute in solvent)	Ostwald solubility L(20.0°C)	Mole fraction solubility x_2(20.0°C)
He in water	0.00937	7.03×10^{-6}
Ar in water	0.0366	2.75×10^{-5}
Xe in water	0.118	8.84×10^{-5}
H_2 in *n*-octane	0.0990	6.64×10^{-4}
Ar in *n*-octane	0.361	2.43×10^{-3}
Xe in *n*-octane	4.38	2.88×10^{-2}

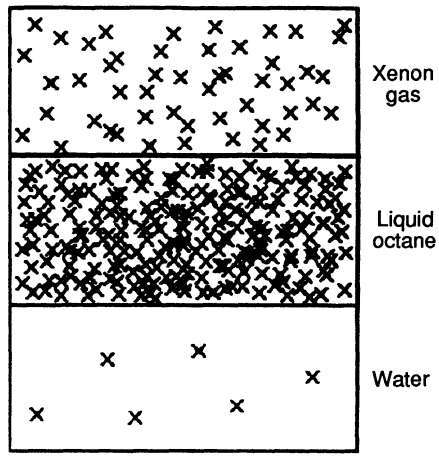

Fig. 1. Schematic representation of the solubility of Xe gas in equal volumes of *n*-octane and water at 20°C. Each × represents an arbitrary number of Xe atoms. For Xe in *n*-octane, a representative nonpolar hydrocarbon liquid, the Ostwald solubility L(20°C) = 4.36 (*24*), and for Xe in water L(20°C) = 0.118 (*5*). Hence, the number densities are related by $\rho_{Xe}^{octane} = 4.36\ \rho_{Xe}^{gas}$, and $\rho_{Xe}^{water} = 0.118\ \rho_{Xe}^{gas}$. The solubility of Xe in olive oil, a representative biological oil, is L(20°C) = 2.0 (*10*).

Nuclear medicine. Preferential solubility of inert gases in nonpolar solvents is applied in nuclear medicine to monitor blood flow to the brain. The principle is that a known amount of ^{133}Xe, a gamma-emitting radioisotope, is introduced into blood flowing into the brain. Because Xe molecules are nonpolar, they diffuse preferentially from blood plasma, which may be considered an aqueous solution, into lipid tissues in the brain, which may be considered a nonpolar solvent, and concentrate there. This buildup of ^{133}Xe is washed out by the subsequent inflow of fresh blood, which initially has no dissolved Xe. From the time course of the emitted radiation intensity for such washin and washout curves, one gets a measure of perfusion.

Gaseous anesthetics. It has been known for a long time that the solubility of gases in oils is closely correlated with anesthetic potency. Olive oil is commonly used in such studies as a prototype for biological oils and lipids (*10*). Figure 3 shows a plot of solubilities for seven gases in olive oil and in water as ordinate versus pressures needed to maintain anesthesia as abscissa. For these seven gases the correlation with solubility in water, approximately $P \propto L^{-2}$, is about as good as the correlation with solubility in olive oil, approximately $P \propto L^{-1}$. The relative solubilities do show that inert anesthetic gases will concentrate in lipid-rich regions such as cell membranes. However, from this consideration alone one cannot construct a detailed theory of the mechanism of anesthesia, because anesthetic pressures also correlate with several other molecular properties of gases. A lot of work has been aimed at finding the primary sites of action of anesthetic gases (*11, 12*).

Deep-sea diving. Solubility of inert gases in body tissues is also important for understanding decompression sickness and inert gas

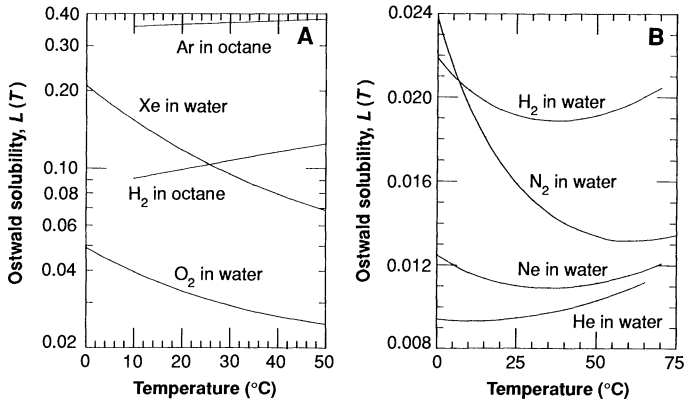

Fig. 2. (**A** and **B**) Temperature dependence of Ostwald solubility for some nonreacting gases in *n*-octane (*9*) and in water (*5*).

Table 2. Ostwald solubilities for O_2 and the anesthetic gases halothane ($C_2HBrClF_3$) and teflurane (C_2HBrF_4) in water, blood, and olive oil (*5, 10, 45*) and for Kr in liquid metals (*46*).

System	Ostwald solubility
O_2 in water	$L(37.0°C) = 0.0272$
O_2 in blood	$L(37.0°C) = 0.0261$
O_2 in olive oil	$L(37.0°C) = 0.133$
Teflurane in water	$L(37.0°C) = 0.32$
Teflurane in blood	$L(37.0°C) = 0.60$
Teflurane in olive oil	$L(37.0°C) = 29$
Halothane in water	$L(37.0°C) = 0.81$
Halothane in blood	$L(37.0°C) = 2.5$
Halothane in olive oil	$L(37.0°C) = 220$
Kr in liquid cadmium	$L(1100°C) \simeq 1.5 \times 10^{-8}$
Kr in liquid lead	$L(900°C) \simeq 1.3 \times 10^{-7}$

narcosis, two important problems in deep-sea diving (*13*). The gas that a diver breathes is a mixture of O_2 and inert gas, usually N_2 or He. Because the total gas pressure must equal the ambient pressure at depth, which can be several or even many atmospheres, and the partial pressure of O_2 must be kept low to prevent O_2 toxicity, the breathing mixture generally consists mainly of inert gas. During a dive these inert gases dissolve under pressure in all tissues of the body, aqueous, fatty, and so forth, so that to avoid decompression sickness the gases must be safely expelled before the diver returns to atmospheric pressure. Gas solubility and diffusion are among the variables that control the rates at which gas concentrations are built up, distributed, and removed in the tissues. The molecular basis of these properties can be used to optimize decompression procedures and other aspects of diving practice.

Nuclear reactor cleanup. Radioactive inert gases are important fission products of U and are emitted from nuclear power plants during normal operation and, in much larger amounts, during reactor accidents (*14, 15*). Probably the two most important of these gases are ^{133}Xe (half-life, 5.25 days) and ^{85}Kr (half-life, 10.8 years), which are, respectively, 6.6% and 0.3% of the fission products of ^{235}U. Because of their volatility and nonreactivity, it is difficult to trap these gases chemically or in filters. However, if the gases are mixed with air in a contained volume, then one can separate and isolate them by use of preferential solubility techniques.

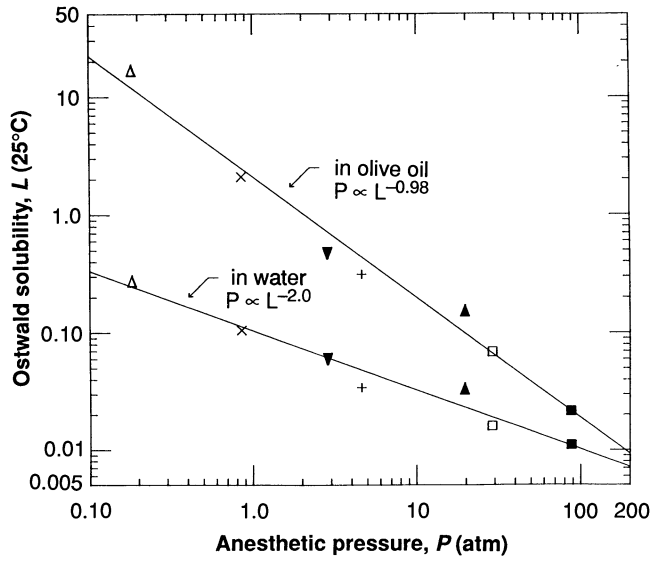

Fig. 3. Ostwald solubilities (ordinate) of seven anesthetic gases plotted against their anesthetic pressures (abscissa): ▲, Ar; +, CH_4; △, c-C_3H_6; ▼, Kr; □, N_2; ■, Ne; ×, Xe. Upper and lower data points are for gas solubility in olive oil (*10*) and water (*5*), respectively. Pressures are approximately those needed for maintenance of anesthesia in a person or animal (*42–44*). For these solvents linear regression applied to the logarithms of both variables gives the equations: $P\,L^{0.98} = 2.06$ and $P\,L^{1.98} = 0.0113$, where L is measured at 25°C and P is in atmospheres. For these gases anesthetic pressures are inversely proportional to the solubilities in olive oil and inversely proportional to the square of the solubilities in water.

Such a technique has been developed at Oak Ridge National Laboratories and proposed for use in the cleanup of the nuclear reactor accident of 1979 at Three Mile Island (TMI-2). As a result of that accident, the reactor's containment building, whose volume is about 5.7×10^7 liters, was contaminated with about 57,000 Ci of ^{85}Kr, or about 1.7 mol or 38 liters (standard temperature and pressure). In order to have safe access to the reactor, it was necessary to remove the radioactive gas from the much larger volume of air with which it was mixed, or to get rid of the radioactive gas some other way. The principle of the technique is to use the preferential solubility of Kr, compared to air, in the slightly polar liquid Freon-12 (CCl_2F_2) at −31°C, just below its boiling point. Under this condition, Kr is about six times as soluble as N_2 and three times as soluble as O_2 in Freon-12. It is possible to separate the radioactive gas with good efficiency, by iteratively passing the contaminated reactor atmosphere through a column of flowing liquid Freon. Although in the actual event of the TMI-2 cleanup this technique was not used, but rather the ^{85}Kr was vented to the atmosphere through a high stack, yet it remains potentially valuable for future applications.

Blood substitutes and oxygen carriers. One important direction in the development of blood substitutes is use of droplets of perfluorochemicals, carried in a suitable aqueous ionic solution, to transport molecules to and from tissues in living systems (*16*). Gas molecules, in this case O_2, concentrate in these nonpolar liquids (*17*), as we have seen. One may therefore picture a gas-carrying blood substitute as a rearrangement of Fig. 1, in which the nonpolar liquid occupies about 20 to 25% of the volume and is distributed throughout the aqueous phase in the form of emulsified spheres about 0.1 μm in diameter.

It is not difficult to calculate the total amount of gas carried by this liquid. If L_P is the Ostwald solubility of a gas in the perfluorochemical, α_P is the fraction of the total liquid volume occupied by perfluorochemical, and L_A and α_A are the corresponding quantities for the aqueous phase, then the Ostwald solubility for the mixture is: $L_{total} = L_P\alpha_P + L_A\alpha_A$. We have neglected the effect of the emulsifier molecules, which typically are about 3% of the volume.

A molecular understanding of gas solubility in liquids may make it possible to design a blood substitute with controlled gas transport, viscosity, body retention, and other properties. These can then be optimized for use in organ preservation, studies of fluid dynamics of circulation, or for whole body circulation.

The subject of hydrophobic interactions (*18*) may be investigated by gas solubility measurements in biological aqueous solutions. One can also use solubility techniques, for example, with Kirkwood-Buff theory, to study interactions between gas molecules and amino acids or other biological molecules (*19*).

Statistical Mechanics of Solubility

When a liquid surface is exposed to a solute gas, gas molecules enter the liquid until the equilibrium number density ρ_2^ℓ, which corresponds to $L(T)$, is reached. This equilibrium is characterized in thermodynamics and statistical mechanics by the condition that the chemical potential for the solute is the same throughout the system. Thus, in Fig. 1, $\mu_{Xe}^g = \mu_{Xe}^{octane} = \mu_{Xe}^{water}$, where μ is the chemical potential. Microscopically one pictures gas molecules impinging on

the interface, at first only from above and then from below also, until the fluxes into and out of the liquid are equal. An understanding of the solution process requires both energetic and probabilistic considerations. For example, an impinging solute molecule cannot in general displace a solvent molecule into the vapor, in other words, it cannot dig its own hole, because its kinetic energy is not large enough. This is so because at room temperature the energy required to remove a molecule from a typical solvent, about 0.7 eV for octane and 0.9 eV for water, is about 30 times the kinetic energy, about 0.026 eV, of a monatomic gas molecule. The conversions from these molecular units to molar units are as follows: 1 eV per molecule equals 96,500 J per mol or 23,100 cal per mol. Part of the solution process is that solute molecules enter the liquid surface at microscopic cavities [whose probability of occurrence is proportional to $\exp(-W/kT)$, where W is the reversible work required to make the cavity and k is the Boltzmann constant] and then diffuse or are stirred into the bulk liquid.

The formal statistical mechanical treatment of gas-liquid solubility (*20*) consists of calculating the chemical potentials for solute molecules in the gas (μ_2^g) and in the solvent phases (μ_2^ℓ) from partition functions, which take into account all the relevant energetic and probabilistic factors. The results are:

$$\mu_2^g = kT \ln \rho_2^g \Lambda^3 \quad (2)$$

and

$$\mu_2^\ell = kT \ln \rho_2^\ell \Lambda^3 + \mu^* \quad (3)$$

In Eqs. 2 and 3, ρ stands for the solute number density in, respectively, gas and solvent, and Λ is the de Broglie thermal wavelength, which comes from the kinetic energy part of the partition functions. The contribution of the solute's internal partition function has been omitted in Eqs. 2 and 3. This is a good approximation for monatomic and other simple solute gases such as those discussed here. For more complex polyatomic solutes, however, the internal partition functions must be included (*20*). Equation 2 and the first term on the right side of Eq. 3 are for an ideal case where there are no solute-solvent or solvent-solvent interactions. But the term μ^*, called the excess chemical potential, comes from the potential energy of solute-solvent and solvent-solvent interactions, which are always present in real solubility problems. In order to connect statistical mechanics with the measurable quantity L of Eq. 1, we apply the equilibrium condition $\mu_2^g = \mu_2^\ell$ to Eqs. 2 and 3 to obtain:

$$\mu^*(T) = -RT \ln L \quad (4)$$

For convenience in later discussions, Eq. 4 is written in molar rather than molecular terms, where $R = N_A k$ is the gas constant in units of joules per mole-kelvin or calories per mole-kelvin.

From its origin in the potential energy part of the partition function, one can interpret the excess chemical potential as the Gibbs free energy required to take one mole of solute atoms from fixed positions in the solute and bring them to fixed positions in the solvent (*20*). With the help of Eq. 4 we can now give a partial answer to the question implied by the title of this article. Gases dissolve in liquids because the reversible work μ^*/N_A required to insert a gas molecule into a liquid is finite; and the smaller μ^*, the larger the solubility. Sometimes, as for nonpolar gases in nonpolar liquids, μ^* is negative so that L is greater than one (*4*). However, even when μ^* is positive and large compared to RT, as for nonpolar noninteracting gases in water, gas dissolves in the solvent. In that case L is much less than one (*5*).

A general approach to predicting solubilities is to calculate μ^* for a particular postulated solubility mechanism, and obtain L from Eq. 4. Probably the most commonly used mechanism, and the principal one we shall consider, consists of two processes: First, make in the solvent a cavity just large enough to fit a solute molecule; the Gibbs free energy associated with this process is called g_{cav}. Second, put a solute molecule into the cavity and consider it to interact with the surrounding solvent molecules; the associated Gibbs free energy is g_{int}. One then has:

$$\mu^*(T) = -RT \ln L = g_{cav} + g_{int} \quad (5)$$

This mechanism has the analytical advantage that it considers the solute-solvent interaction potential in two parts. The first process treats the short-range repulsive part of the potential, and the second process involves the rest of the potential, the attractive, long-range, soft part (*21, 22*).

One can gain some insight from Eq. 5 into why many nonreacting gases are much less soluble in water than in nonpolar liquids. In general for model calculations, $g_{cav} > 0$, $g_{int} < 0$, and the cavity energies in water are indeed much larger than in nonpolar liquids. Thus one can argue that gases are generally more soluble in D_2O than in H_2O because g_{cav} is smaller in D_2O, because it has a somewhat more open structure than H_2O. In the same way, the large solubility of CO_2 in water is partly a result of a large and negative g_{int}, and so forth. However, such intuitive arguments must be used with caution because entropic contributions to the Gibbs free energies are important and often difficult to calculate or even to estimate.

Even for an ideal gas, where there are no attractive forces, the contribution of entropy is large and hard to understand intuitively. Thus, if one applies Eq. 2 to Xe gas at 20°C and 1 atm, as in Fig. 1, then one obtains for the chemical potential $\mu_2^g = -17.9\,kT$ (−0.45 eV per molecule). Since $\mu = g = u + Pv - Ts$, the entropic contribution to μ is $-Ts$. It can be obtained with the Sackur-Tetrode equation (*23*), as $-20.4\,kT$ for this case, so that it dominates the reversible work. The rest of μ, the enthalpic contribution $h = u + Pv$, is just $2.5\,kT$.

Some more insight into solubility comes from restating Eq. 5, in thermodynamic terms. If V_2 is the partial molar volume of solute in the solvent, V_2^g is the molar volume in the gas, and ϕ_2 is the volume fraction of the solution that is occupied by solute, then $L = \phi_2 V_2^g / V_2$ and Eq. 5 becomes:

$$g_{cav} + g_{int} - RT \ln (V_2/V_2^g) + RT \ln \phi_2 = 0 \quad (6)$$

We interpret Eq. 6 to mean that the total Gibbs free energy for transferring 1 mol of solute into the solvent is the zero sum of four terms. The first two terms are for the processes described above. The third term is the energy associated with isothermal and reversible compression of the solute from its volume in the gas to its volume in solution. The last term may be interpreted as the free energy associated with the mixing entropy $-R \ln \phi_2$ in a real solution. In words, solute molecules dissolve in the solvent up to that volume fraction ϕ_2 for which the associated free energy change is enough to overcome the free energies for the processes of the first three terms.

Experiments on Simple Solute-Solvent Systems

In this section I apply the theory to results of experiments on prototype solute-solvent systems, in order to see how far it can carry us toward the first-principles understanding we seek. I discuss here chiefly experiments with Xe gas as solute and organic liquids chosen from six homologous series as solvents (*17, 24–26*).

Xenon has several properties that justify its use as a simple solute, for example, it is monatomic, spherical in the ground state with an

outermost completed p electron shell, and inert. The interatomic potential between Xe atoms is a van der Waals potential with a characteristic well depth ϵ and hard-core diameter of interaction σ (ϵ/k = 228 K, σ = 3.973 Å) that is comparatively well understood (*27*). Inert gas elements have been used extensively as prototype solids and liquids (*27–29*); I use them here as prototype solutes. Xenon, in particular among the inert gases, recommends itself for these experiments because it has a radioactive isotope, ^{133}Xe, which is easily detected and commercially available.

The solvents that were used for these experiments, 45 solvents in all, were: (i) all normal alkanes from n-C_5H_{12} to n-$C_{20}H_{42}$ (*24*), (ii) 13 of the normal alkanols from CH_3OH to n-$C_{14}H_{29}OH$ (*25*), (iii) six normal carboxylic acids from formic to n-hexanoic acid, (iv) four normal alkanals from propanal to n-heptanal, (v) cyclopentane, -hexane, and -octane (*26*), and (vi) perfluoroheptane, -hexane, and -octane (*17*). The strategy of this choice of solvents is that the molecules within each homologous series differ from each other in a controlled way, by a CH_2 or CF_3 group, for instance, and the molecules of each series differ from their analog molecules in the other series in a controlled way. This paradigmatic chemical physics strategy is suggested by the idea that L and, especially, μ^* in Eq. 5 can be considered as built up from individual contributions from functional groups. Another consideration is that these solvents, at room temperature, range in steps from large nonpolar molecular liquids (n-hexadecane) to liquids with small polar molecules for which hydrogen bonding is important (CH_3OH and HCOOH).

Complementary to this work with a solute of gaseous Xe, and in the same reductionist spirit, is an experiment of Rentzepis and Douglass on the properties of liquid Xe at room temperature as a solvent for several biological and organic molecules (*30*), and work of Halsey and co-workers in which liquid Ar was used at low temperatures as a solvent for He, Ne, and H_2 gas (*31*).

Figure 4 shows the results of measurements of Xe solubility in six representative solvents, one from each series. These measurements are of Ostwald solubility in the limit of low solute pressure; the partial pressure of ^{133}Xe was typically of the order of picoatmospheres. Equation 4 was used to calculate values of $\mu^*(T)$ from the actual $L(T)$ data, so that the range of the data shown in Fig. 4 runs from L(50°C, n-hexanol) = 1.92, the lowest value, to L(10°C, n-hexane) = 5.91, the highest value.

For all the solvents in Fig. 4, $\mu^*(T)$ increases linearly (that is, it becomes less negative) as T increases. That means that less work is needed to remove a solute molecule from a hot solvent than from a cold one. The straight lines shown are of the form $\mu^*(T) = a + bT$, with a and b constant. One can also write this as $\mu^*(T) = h^* - Ts^*$, where h^* is the excess enthalpy of solvation and s^* is the excess entropy of solvation over the temperature interval.

One of the remarkable features of the data in Fig. 4 is that the lines for all the solvents have nearly the same slope. This implies that the s^* values are almost the same. In fact, the values of s^* for all the solvents we investigated were remarkably independent of solvent; the average over all 45 solvents was $s^*_{average} \pm SD = -4.1 \pm 0.5$ cal mol^{-1} K^{-1}. The negative value of s^* is associated with solvent ordering, and its constancy implies that, when a Xe atom is solvated in any of these solvents, in some sense the amount of ordering is the same. It is reasonable to expect that the s^* associated with solvation of other noninteracting solutes, at least nonpolar ones, in solvents like ours will also be constant. It would be interesting to compare the values of s^* with the molecular dimensions of the corresponding solutes. The entropy of hydration for Xe, taken from solubility data in water in about the same temperature range (*32*), is -18 cal mol^{-1} K^{-1}. This suggests a higher degree of solvent ordering for Xe in water than in other solvents, probably due to the polarizability of Xe, dipole-dipole interactions, and hydrogen bonding. Hildebrand *et al.* (*2*) discussed the entropy of solution, on the mole-fraction scale, in terms of the solubility of many gases in a single solvent, particularly cyclohexane.

From data such as those of Fig. 4, one can obtain values of h^* as the intercept of $\mu^*(T)$ at T = 0 K. The value of $h^*_{average} \pm SD$ for Xe, averaged over these solvents (formic acid excluded), was -1840 ± 250 cal mol^{-1}, and the value of h^* for Xe in water is -4050 cal mol^{-1}. In general in solubility systems at low pressure, the value of h^* is dominated by the internal energy of solute-solvent interaction, that is, $h^* \approx u^*$, so that a negative and large-magnitude value for h^* reflects a relatively tight binding between solute and solvent due to the potential energy of interaction.

We can now give a first answer to the question posed earlier on temperature dependence of solubility, in the following way: Solve Eq. 4 for $L(T)$, substitute $\mu^*(T) = h^* - Ts^*$, assume that h^* and s^* are constants over the temperature interval of interest, and differentiate, to obtain the relation $dL/dT = Lh^*/RT^2$. This equation means that the temperature dependence of L is determined by the average value of h^* in the interval. Thus from data such as the $L(T)$ curves in Fig. 2, one can determine the sign of h^*. For all of our solute-solvent systems, h^* is negative in the temperature intervals of the experiments. Therefore, in these intervals, $L(T)$ decreases with temperature for them.

A characteristic of Xe solubility in these solvents is that the solvation process is enthalpically dominated; for 44 of our solvents the average value of $h^*/Ts^* = 1.5 \pm 0.15$. In contrast, Xe solubility in water is entropically dominated because in water $h^*/Ts^* = 0.75$ (*32*). One may say that L for Xe in water is small because the large, positive contribution of s^* dominates μ^*.

An interesting sidelight of these data is that the solubility properties of formic acid are in some ways similar to those of water. The solvation of Xe in formic acid is entropically dominated and the Ostwald solubilities are less than one, for example, L(20°C, Xe in HCOOH) = 0.46. Carboxylic acids offer a kind of bridge from the nonpolar solvent behavior of long-chain fatty acids to the waterlike behavior of formic acid.

Analytical and Computer Simulation Approaches to Solubility

We have seen that the solubility of a gas in a liquid depends on the equilibrium of Gibbs free energies and also that the actual value of the Ostwald solubility can be determined by calculation of μ^*. Microscopic properties on which μ^* depends are the solute-solvent and solvent-solvent interaction potentials, as well as the solute-solvent distribution function, all of which in general depend on molecular arrangements in a complicated way. Unfortunately, all the ways of calculating chemical potentials in liquids are more or less difficult, even for pure liquids (*33*). In this section I will first discuss calculations for μ^* that use Eq. 5 and then, more briefly, other approaches.

Cavity energy. In order to obtain $\mu^*(T)$, or $L(T)$, from Eq. 5, one must calculate g_{cav} and g_{int}. The Gibbs energy to produce a cavity in a solvent can be calculated from the scaled-particle theory of liquids (*34*). Results of such calculations for Xe in six solvents are shown in Fig. 5 (*26*).

Scaled-particle theory is a versatile, formal theory that has provided many successful predictions and insights. In scaled-particle theory one characterizes the solvent by a hard-sphere molecular diameter a_1, which is determined from the heat of vaporization and thermal expansivity of the solvent. Calculation of spherical diameters for long-chain and polar molecules, such as those in our solvents, is an application of scaled-particle theory well beyond the spherical

molecules for which it was originally intended. Thus, for example, a_1 for *n*-dodecane is 7.62 Å by this procedure, whereas the usual C–C bond length is 1.5 Å. However, it is interesting to note that when one uses a spherical approximation in other, more modern, estimations of molecular size the hard-sphere diameters are close to those obtained from scaled-particle theory. For example, a value of 7.53 Å was recently obtained for *n*-dodecane, from the use of a Carnahan-Starling equation of state with molecular dynamics simulations (*35*).

The values of g_{cav} shown in Fig. 5 are the cavity Gibbs energies required to produce in the solvent N_A cavities of radius $r_{12} = (a_1 + a_2)/2$, where $a_2 = 3.97$ Å, the hard-core diameter of a Xe atom. In scaled-particle theory one obtains the expression for this energy by scaling between a microscopic cavity, associated with the probability $\exp[-W(r)/kT]$, and the energy to make a macroscopic cavity, which depends on the surface tension of bulk solvent. The cavity energies in Fig. 5 are positive and decrease with increasing temperature—it is easier to make a cavity in a hot solvent than in a cold one.

One can calculate the enthalpies of cavity formation h_{cav}, where $g_{cav} = h_{cav} - Ts_{cav}$, from the cavity Gibbs energies by using the Gibbs-Helmholtz equation: $h_{cav} = -T^2[\partial(g_{cav}/T)/\partial T]_P$. The enthalpies do vary systematically with the solvent structure and seem to be physically significant for other reasons as well. However, the same cannot be said for the entropies of cavity formation, s_{cav}. The difficulty may be that the values currently available for thermal expansivities of these solvents are not good enough (*26*).

Interaction energy. The term g_{int} in Eq. 5 is the Gibbs energy associated with interaction of solute molecules with solvent after they have been placed in the cavities. As usual, this energy may be written in terms of an enthalpic contribution h_{int} and an entropic contribution s_{int} as: $g_{int} = h_{int} - Ts_{int}$. One can calculate h_{int}, approximately, from the soft part of the solute-solvent potential; it is essentially the internal energy of the system. However, s_{int} is much more difficult to calculate and we shall not attempt that here. Instead we do the next best thing.

Figure 6 shows values for the reduced interaction Gibbs energy, g_{int}/ρ_1, for 37 of our solvents at 25°C. These values were obtained by solving Eq. 5 for $g_{int} = -RT \ln L - g_{cav}$; that is to say, they are calculated from a combination of both experimental data, for L, and computed values, for g_{cav}. Put yet another way, the Gibbs energies of interaction used in Fig. 6 are the values g_{int} would have if Eq. 5, the $L(T)$ data, and calculated values for g_{cav} were all rigorously correct. It is important to point out that the g_{int} values on the ordinate have been reduced by division by the solvent number density ρ_1. This reduction is useful for two reasons: The fundamental reason is that expressions for calculating g often are proportional to ρ_1 as, for example, Eq. 8 below. The practical reason is that it supports an empirical approach. The abscissa for Fig. 6 is the number of CH_2 groups in the solvent molecule.

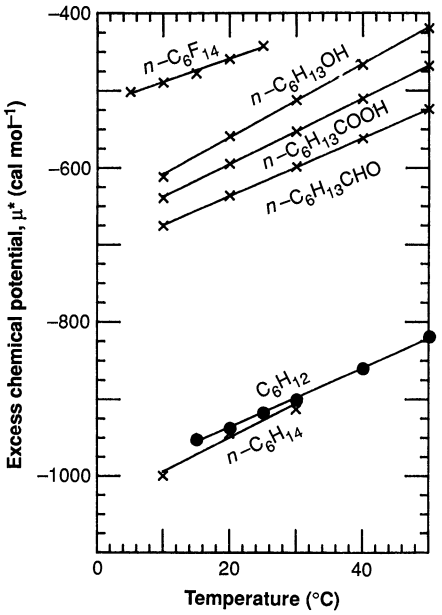

Fig. 4. Solubility results, in the temperature range 5° to 50°C, for Xe gas at low pressure in six organic solvents. Data were taken from (*17, 24–26*). The ordinate μ^* is related to Ostwald solubility L by $\mu^* = -RT \ln L$, Eq. 4, and related to the excess enthalpy h^* and excess entropy s^* by $\mu^* = h^* - Ts^*$. The conversion between the macroscopic units on the ordinate axis and microscopic units is 1000 cal mol^{-1} = 0.043 eV per molecule. [Adapted from (*26*) with permission of the American Institute of Physics, copyright 1989]

It is natural to use Fig. 6 for empirical predictions of solubility of Xe, because the data for each homologous series of solvents lie on straight lines, which are nearly parallel. The slopes of these lines are the empirical contribution, which we call $\gamma_i(CH_2)$, for each CH_2 group in the solvent to the g_{int} for Xe in that solvent. If one carries this procedure through, one obtains $\gamma_i(CH_2, \text{linear}) = -106.5$ (cal mol^{-1})/(mol $liter^{-1}$) as the average slope for the linear solvents, and $\gamma_i(CH_2, \text{cyclo}) = -96.6$ as the slope for the three cycloalkanes. The intercepts on the ordinate axis of the lines through the data for each solvent in Fig. 6 give the contributions of the other functional groups. Thus, for example, the *n*-alkane intercept corresponds to the contribution of two methyl groups, so that $\gamma_i(CH_3) = -74.0$ for each CH_3. The intercept for the cycloalkane data is essentially zero, as it should be if this procedure is to be consistent.

One uses these values to predict solubilities, say, for a normal alkanal with m CH_2 groups, in the following way. One obtains an estimate of the Gibbs energy of interaction from $g_{int} = \rho_1[\gamma_i(CH_3) + m\gamma_i(CH_2) + \gamma_i(CHO)]$, calculates a value for g_{cav} from scaled-particle theory or otherwise, and obtains L from substitution in Eq. 5. This procedure could be extended to other functional groups by solubility measurements on other solvents, such as aromatic solvents, esters, ketones, and halogenated solvents, as well as to other solutes. Its ultimate usefulness depends on whether g_{int} can indeed be made up of additive contributions from functional groups, and also, of course, on how meaningful calculated values of g_{cav} are for complex solvents. Jorgensen and co-workers have constructed optimized potentials for several groups on hydrocarbons and achieved good results using them in liquid simulations (*36*). That work supports the principle of building up contributions to the chemical potential. An analogous empirical procedure, described by Pollack *et al.* (*26*), depends only on the experimental quantities μ^*, h^*, and s^*.

Other approaches. A particularly interesting and general method for calculating chemical potential is the charging technique of Onsager and Kirkwood (*37*). In this approach, the expression one uses for excess chemical potential of a solute molecule in a solvent is:

$$\mu^*/N_A = -kT \ln L = \rho_1 \int_0^1 d\xi \int_V g_{12}(\mathbf{r},\xi)\, \phi_{12}(\mathbf{r})\, d^3\mathbf{r} \qquad (7)$$

In Eq. 7, g_{12} is the solvent-solute pair distribution function, ϕ_{12} is the solvent-solute interaction potential, $\mathbf{r}$ is the vector from the solute molecule into the solvent, and V is the volume. The parameter ξ couples the solute molecule to the solvent, so that, as ξ grows from zero to one, the solute-solvent coupling grows from noninteracting to fully interacting.

Techniques of this kind have been used for molecular dynamics (*38*) and Monte Carlo (*39*) calculations of the chemical potential of simple solutes in water. For calculations of free energies, or indeed for almost any liquid state calculations, water has the advantages that it is the most investigated of all solvents and several good interaction potentials are available for it. In computer simulations of this kind, one uses Eq. 7 in the form

$$-kT \ln L = \int_0^1 U(\xi)\, d\xi \qquad (8)$$

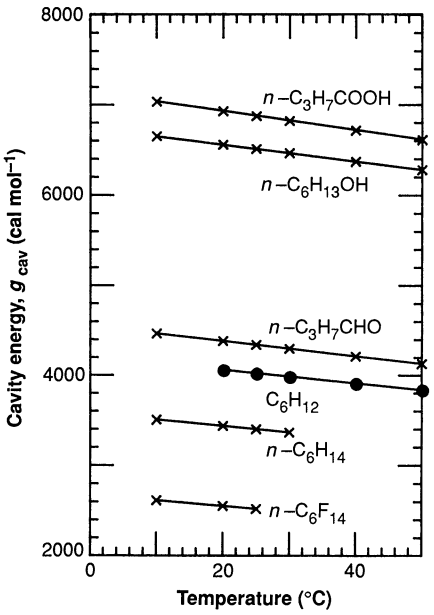

Fig. 5. The ordinate is the Gibbs free energy for making in a solvent N_A cavities each large enough for a Xe atom. Values for g_{cav} were calculated from scaled-particle theory of liquids, in which each solvent molecule is characterized by a hard-sphere diameter obtained from the solvent's heat of vaporization and thermal expansivity. [Adapted from (*26*) with permission of the American Institute of Physics, copyright 1989]

where $U(\xi)$ is an averaged interaction potential, at the coupling strength ξ, for a solute molecule with the entire solvent. One therefore does not need an explicit distribution function; rather $g_{12}(\mathbf{r},\xi)$ is obtained from the simulation.

Conclusions

Our present understanding of the solubility of gases in liquids is based on arguments and equations from statistical mechanics and thermodynamics that have been tested on many systems. Theoretical calculations can be carried out that give good qualitative, and sometimes quantitative, predictions of solubility, especially in simple systems. The most practical way of predicting solubility in an arbitrary gas-liquid system is to use empirical and correlational techniques together with modern arguments based on microscopic properties of solute and solvent.

As I have shown, solubility calculations inevitably involve calculations of chemical potential. One of the interesting ways to do this analytically is with Eq. 7, which requires functions that describe the solute-solvent distribution and potential of interaction. For complex solutes and solvents, or even for the relatively simple systems discussed in this article, these two functions are difficult to obtain analytically from microscopic principles. Fortunately, good interaction potentials are now available for several of the functional groups of which solvents and solutes are composed, and it is likely that such potentials will soon be available for many more groups. The distribution function that is needed to describe a complex system depends on many variables, namely, those that describe intramolecular as well as intermolecular configurations. Fortunately, for many systems the solute-solvent interactions are dominated by the close-in configurations and there are experimental techniques for obtaining some of these.

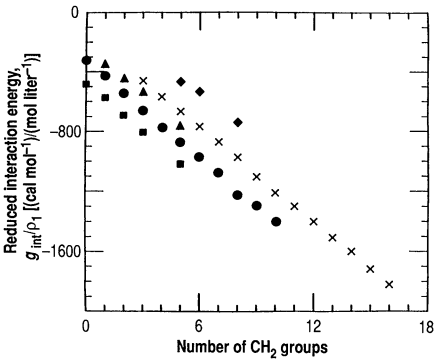

Fig. 6. Interaction Gibbs free energies, g_{int}, for Xe solvation plotted as a function of the number of CH_2 groups in the solvent molecule. Results for 37 solvents are shown, namely, all n-alkanes (x) from n-C_5H_{12} to n-$C_{18}H_{38}$, all n-alkanols (●) from CH_3OH to n-$C_{11}H_{23}OH$, five carboxylic acids (■) from CH_3COOH to n-$C_6H_{13}COOH$, four alkanals (▲) from C_2H_5CHO to n-$C_6H_{13}CHO$, and three cycloalkanes (◆) (*26*). The g_{int} values were obtained from $g_{int} = -RT \ln L - g_{cav}$. The ordinate has been reduced by division by ρ_1, the solvent number density. [Adapted from (*26*) with permission of the American Institute of Physics, © 1989]

A fundamental problem in calculating chemical potentials is that they always have an entropic contribution, which is, in general, important as well as difficult to calculate. One of the main reasons for using the coupling parameter approach, as in Eq. 7, is to fold in the entropic contribution. An important outstanding problem then is to calculate entropy from first principles for real solute-solvent systems. This may be easier than appears since s^* may vary only a little over many solvents. Ideally one would like to know how to calculate s^* in general, but it would also be interesting to have calculations of model-dependent entropies, such as the entropies of interaction, s_{int}, or of cavity formation, s_{cav}.

Another way to calculate solubilities for solute-solvent systems is with computer simulations, such as have been successfully applied to problems of solubility in water. The same techniques can work for solubility in general systems if one can take proper account of complicated geometry and interaction potentials. Another strategy for sharpening our understanding of interactions in solute-solvent systems is to use computer simulations to calculate molecular diffusion. Diffusion is a property of solute-solvent systems that is closely related to solubility in several applications. Diffusion also depends on interaction potentials and molecular configurations but does not depend explicitly on the chemical potential. Its calculation is, at least in that sense, more straightforward. There have been recent measurements, which can be used for this purpose, of molecular diffusion in some of the same systems discussed here (*40, 41*). Underlying the discussion of the preceding three paragraphs is the question: What are the inherent advantages of analytical compared to simulational calculations of chemical potential and other thermodynamic quantities?

Most of the solubility experiments I have discussed are on relatively simple systems, but there are organic solvents with even simpler structures, for example, some such as ethane and methane that are gases at low pressure near room temperature. One can, using cryogenic techniques, design experiments to measure solubility of radioactive isotopes of inert gases in these and other volatile organic solvents. The inert gases Xe, Kr, and Rn all have isotopes suitable for such experiments, namely, ^{133}Xe, ^{85}Kr, and ^{222}Rn. Although these solutes have triple point temperatures that are higher than methane's, one could measure their solubilities using tracer techniques at partial pressures around the milliatmosphere range and lower, at which the solutes would not condense (*27*). Such cryogenic solute-solvent systems would be amenable to simpler theoretical treatment than room temperature systems.

REFERENCES AND NOTES

1. W. Henry, *Philos. Trans. R. Soc. London* **93**, 29 (1803); *ibid.*, p. 274.
2. J. H. Hildebrand, J. M. Prausnitz, R. L. Scott, *Regular and Related Solutions* (Van Nostrand Reinhold, New York, 1970).
3. R. C. Reid, J. M. Prausnitz, B. E. Poling, *The Properties of Gases and Liquids* (McGraw-Hill, New York, ed. 4, 1987).
4. R. Battino and H. L. Clever, *Chem. Rev.* **66**, 395 (1966).
5. E. Wilhelm, R. Battino, R. J. Wilcock, *ibid.* **77**, 219 (1977).
6. R. Battino, *Fluid Phase Equilib.* **15**, 231 (1984).
7. R. Fernández-Prini, R. Crovetto, M. L. Japas, D. Laria, *Acc. Chem. Res.* **18**, 207 (1985).
8. R. P. Kennan and G. L. Pollack, *J. Chem. Phys.* **93**, 2724 (1990).
9. E. Wilhelm and R. Battino, *Chem. Rev.* **73**, 1 (1973).
10. P. Seeman, *Pharmacol. Rev.* **24**, 583 (1972).
11. B. R. Fink, Ed., *Molecular Mechanisms of Anesthesia* (Raven, New York, 1975).

12. N. P. Franks and W. R. Lieb, *Nature* **274**, 339 (1978); *ibid.* **316**, 349 (1985).
13. P. B. Bennett and D. H. Elliott, Eds., *The Physiology and Medicine of Diving* (Baillière Tindall, London, ed. 2, 1975).
14. C. O. Kunz and C. J. Paperiello, *Science* **192**, 1235 (1976).
15. U.S. Nuclear Regulatory Commission (NRC), Report NUREG-0662 (March 1980); G. L. Pollack, NRC Accession No. 8008190073 (September 1979); NRC Accession No. 8004160039 (March 1980).
16. K. C. Lowe, Ed., *Blood Substitutes* (Horwood, Chichester, England, 1988); T. M. S. Chang and R. P. Geyer, Eds., *Blood Substitutes* (Dekker, New York, 1989).
17. R. P. Kennan and G. L. Pollack, *J. Chem. Phys.* **89**, 517 (1988).
18. A. Ben-Naim, *Hydrophobic Interactions* (Plenum, New York, 1980).
19. G. L. Pollack and J. F. Himm, *J. Chem. Phys.* **85**, 456 (1986); R. P. Kennan, J. F. Himm, G. L. Pollack, *ibid.* **88**, 6529 (1988); *Bull. Am. Phys. Soc.* **35**, 500 (1990).
20. A. Ben-Naim, *Solvation Thermodynamics* (Plenum, New York, 1987).
21. D. Chandler, J. D. Weeks, H. C. Andersen, *Science* **220**, 787 (1983).
22. J. P. Hansen and I. R. McDonald, *Theory of Simple Liquids* (Academic Press, London, ed. 2, 1986).
23. C. Kittel and H. Kroemer, *Thermal Physics* (Freeman, New York, 1980).
24. G. L. Pollack, *J. Chem. Phys.* **75**, 5875 (1981); _____ and J. F. Himm, *ibid.* 77, 3221 (1982).
25. G. L. Pollack, J. F. Himm, J. J. Enyeart, *ibid.* **81**, 3239 (1984).
26. G. L. Pollack, R. P. Kennan, J. F. Himm, P. W. Carr, *ibid.* **90**, 6569 (1989).
27. G. L. Pollack, *Rev. Mod. Phys.* **36**, 748 (1964).
28. M. L. Klein and J. A. Venables, Eds., *Rare Gas Solids* (Academic Press, London, 1976, 1977), vols. I and II.
29. H. L. Frisch and Z. W. Salsburg, Eds., *Simple Dense Fluids* (Academic Press, New York, 1968).
30. P. M. Rentzepis and D. C. Douglass, *Nature* **293**, 165 (1981).
31. F. E. Karasz and G. D. Halsey, Jr., *J. Chem. Phys.* **29**, 173 (1958); H. Volk and G. D. Halsey, Jr., *ibid.* **33**, 1132 (1960).
32. B. B. Benson and D. Krause, Jr., *ibid.* **64**, 689 (1976); D. Krause, Jr., and B. B. Benson, *J. Solution Chem.* **18**, 823 (1989).
33. G. L. Deitrick, L. E. Scriven, H. T. Davis, *J. Chem. Phys.* **90**, 2370 (1989); O. E. Kiselyov and G. A. Martynov, *ibid.* **93**, 1942 (1990).
34. H. Reiss, H. L. Frisch, J. L. Lebowitz, *ibid.* **31**, 369 (1959); H. Reiss, H. L. Frisch, E. Helfand, J. L. Lebowitz, *ibid.* **32**, 119 (1960); R. A. Pierotti, *J. Phys. Chem.* **67**, 1840 (1963).
35. D. Ben-Amotz and D. R. Herschbach, *J. Phys. Chem.* **94**, 1038 (1990).
36. W. L. Jorgensen, J. D. Madura, C. J. Swenson, *J. Am. Chem. Soc.* **106**, 6638 (1984).
37. L. Onsager, *Chem. Rev.* **13**, 73 (1933); J. G. Kirkwood, *J. Chem. Phys.* **3**, 300 (1935); T. L. Hill, *Statistical Mechanics* (McGraw-Hill, New York, 1956).
38. W. C. Swope and H. C. Andersen, *J. Phys. Chem.* **88**, 6548 (1984); K. Watanabe and H. C. Andersen, *ibid.* **90**, 795 (1986).
39. W. L. Jorgensen, J. F. Blake, J. K. Buckner, *Chem. Phys.* **129**, 193 (1989).
40. G. L. Pollack, *Phys. Rev. A* **23**, 2660 (1981); _____ and J. J. Enyeart, *ibid.* **31**, 980 (1985); G. L. Pollack, R. P. Kennan, J. F. Himm, D. R. Stump, *J. Chem. Phys.* **92**, 625 (1990).
41. S.-H. Chen, H. T. Davis, D. F. Evans, *J. Chem. Phys.* 77, 2540 (1982).
42. S. L. Miller, *Proc. Natl. Acad. Sci. U.S.A.* **47**, 1515 (1961).
43. K. W. Miller, W. D. M. Paton, E. B. Smith, *Nature* **206**, 574 (1965).
44. A. Goldstein, L. Aronow, S. M. Kalman, *Principles of Drug Action* (Wiley, New York, ed. 2, 1974).
45. P. K. Weathersby and L. D. Homer, *Undersea Biomed. Res.* 7, 277 (1980).
46. G. W. Johnson and R. Shuttleworth, *Philos. Mag.* **4**, 957 (1959); G. W. Johnson, *ibid.* **6**, 943 (1961).
47. This work was supported by the Office of Naval Research and the Naval Medical Research and Development Command (contract N00014-88-K-0287). I thank R. Battino, A. Ben-Naim, P. W. Carr, R. Fernández-Prini, and E. Wilhelm for helpful discussions. I especially thank my former students R. Kennan and J. F. Himm for all their explanations and other essential help with this work.

Peptide Processing and Targeting in the Neuronal Secretory Pathway

LINDA J. JUNG AND RICHARD H. SCHELLER

The abdominal ganglion of the marine mollusk *Aplysia* contains a pair of identified neuronal clusters, the bag cells, which control egg laying by means of a number of unique regulatory mechanisms. Each neuron in the bag cell clusters synthesizes several peptides derived from a single prohormone and packages them into separate vesicles. These vesicles are then differentially localized in specific neuronal processes, thus segregating peptides destined for autocrine and hormonal release sites. Therefore in this system, protein trafficking through the secretory pathway organizes multiple peptide neurochemical messengers to efficiently regulate simple behaviors.

UNDERSTANDING THE NEURAL AND ENDOCRINE MECHANISMS that govern animal behavior is a major goal of modern biology. Although considerable information has been amassed in molecular, cellular, physiological, and behavioral studies, it has proven difficult to integrate these various levels of investigation into a unified account of behavior. The primary obstacles to such an integration are the complexity of the behaviors of higher animals and the diversity of the underlying cellular and biochemical mechanisms. In an effort to circumvent some of these obstacles, investigators have turned to invertebrate species, many of which have simpler nervous systems and a limited repertoire of elementary behaviors. This approach has proven fruitful.

The authors are in the Howard Hughes Medical Institute, Department of Molecular and Cellular Physiology, Beckman Center, Stanford University, Stanford, CA 94305.

Aplysia as a Behavioral Model

Some molluscan species have distinct advantages for studies of the nervous system, one of which is the fact that many of the nerve cells are very large and reproducibly identifiable among individuals. This characteristic has been exploited in the marine snail *Aplysia californica*, in which both mating and egg laying are highly stereotyped behaviors (Fig. 1) (*1–4*). *Aplysia* are non–self fertilizing hermaphrodites and often mate in groups in which each individual both donates and receives sperm (*5*). The gametes traverse a complex pathway through the reproductive tract where they are fertilized, encapsulated, and finally packaged into a long strand, or cordon (*5, 6*), which contains several million eggs (*1, 6*). The egg strand exits the internal portions of the reproductive tract through a genital aperture in the mantel cavity and then moves along the genital groove toward the head where a series of head waving and tamping movements coil the egg cordon in an irregular compact mass (*2–6*). In this article, we discuss the neural and endocrine factors that govern egg-laying behavior and mating, a social behavior.

Egg-laying behavior is neurally controlled by the bag cells, a set of 800 electrically coupled cells grouped into two clusters along the rostral aspect of the abdominal ganglion (Fig. 5) (*7–12*). When extracts or released material from these neurons are injected into a